2009 American Control Conference
Hyatt Regency Riverfront, St. Louis, MO, USA
June 10-12, 2009

Swarm Coordination under Conflict

Daniel A. Sierra, *Student Member, IEEE,* Paul McCullough, Eldridge Adams, Nejat Olgac, *Fellow, ASME, Senior Member, IEEE*

Abstract— **We consider the conflict dynamics between two multi-agent swarms. First, the complex nature of a single pursuer attempting to intercept a single evader (1P-1E) is investigated, and some rudimentary rules of engagement are established. We elaborate on the stability repercussions of these rules. Second, we extend the modeling and stability analysis to multi-agent swarms. The present document considers only swarms with equal membership strengths for simplicity.**

Due to the strong nonlinearities in the dynamics, Lyapunov-based stability analysis is used. Swarm interactions are taken in two phases: the approach phase during which the two swarms act like individuals in the 1P-1E interaction; and the individual pursuit phase where each pursuer is assigned to an evader.

I. Introduction

This study addresses the modeling analysis and control of multi-agent swarm dynamics of non-alike members. Most earlier investigations that focus on this general theme consider homogenous swarms, *i.e*., those composed of alike members [1-4].

Gazi and Passino [2] contribute to the study of foraging social swarms, where the agents move into a profile of nutrients. Chu et al. [5, 6] address the stability analysis of anisotropic (asymmetric behavior) but non-hostile swarms. They propose some aggregation rules for swarms with reciprocal and non-reciprocal interactions between agents. In the present paper, we extend the application of asymmetric momenta to hostile swarm interactions, which are currently poorly understood.

A number of other groups have also expanded the understanding of swarm aggregation. Chen et al. [7] consider cases in which the motion decision of each agent is based only on the information about its own neighbors or the leader. In Yao et al. [8], the swarm in a formation is guided to track a target. The principal aim is to form a decentralized formation control taking into account the sensory limitation. Kumar and coworkers [9,10] investigate the dynamic coordination of multiple robots to perform cooperative tasks. They use a hybrid systems framework to model the cooperative tasks and dynamic role assignment among multiple robots.

We address an understudied aspect of swarm coordination by including two groups of antagonistic swarm members. In particular, we consider the pursuit of a swarm of "evaders" by a swarm of "pursuers," an operation that includes heterogeneous agents and hostile interactions. Due to the asymmetric governing dynamics, as well as the pursuer/evader assignment policies, the control and stability become quite complex. For simplicity, within this study, we consider only cases with equal numbers of pursuers and evaders.

This paper addresses the governing dynamics of heterogeneous swarms, deploying models of interaction similar to those previously adopted for homogenous swarms [1]. The major novelty is the introduction of heterogeneity in the form of two hostile swarms, which is described in Section II. Pursuer control is partitioned into two phases: group approach and individual pursuit. A Lyapunov based control is introduced in Section III to expedite the capture of the evaders. An example is presented in Section IV to display the efficiency of the capture. Conclusions and discussions suggest the future steps in this research.

II. Swarm Interaction Strategies and a Lyapunov Based Control

A. Analysis of the 1 pursuer-1 evader (1P-1E) scenario

Consider a single member pursuer-evader interaction based on the momentum profiles governed by the dynamics adapted from [1]:

$$\begin{aligned} \dot{x} &= g_{pe}(y) = -yb_{pe}\exp\left(-\|y\|^2/c_{pe}\right) \\ \dot{z} &= g_{ep}(y) = -yb_{ep}\exp\left(-\|y\|^2/c_{ep}\right) \end{aligned} \quad (1)$$

where x and z denote the local vectors of pursuers and evaders (both taken as points), respectively. Vectors $y = x - z$, connect evaders and pursuers. Notation $g_{pe}(.)$ in (1) refers to the momentum received by the pursuer due to the evader. Likewise, $g_{ep}(.)$ is the momentum received by the evader due to the pursuer.

Manuscript received September 9, 2008. This work was supported in part by ARO W911NF-07-1-0557.

D. A. Sierra is with the Biomedical Engineering Department at University of Connecticut, Storrs, CT 06269 USA, and with the Electrical and Electronic Engineering School at *Universidad Industrial de Santander (Colombia)* (e-mail:dasierra @ engr.uconn.edu).

P. McCullough and Nejat Olgac are with the Mechanical Engineering Department, University of Connecticut, Storrs, CT 06269-3139. USA (e-mails: ptm02002 @ engr.uconn.edu and Olgac @ engr.uconn.edu).

E. Adams is with the Ecology and Evolutionary Biology Department, University of Connecticut, Storrs, CT 06269-3139. USA (e-mail: eldridge.adams @ uconn.edu).

Notice that $g_{pe}(.)$ is an *attraction* momentum and $g_{ep}(.)$ is a *repulsion* momentum. Both g_{pe} and g_{ep} diminish as $y \to 0$ (surrender) and $y \to \infty$ (unrecognized presence of other agents). The peak, $g_{pe\_\max} = b_{pe}\sqrt{c_{pe}/2}\exp(-1/2)$, occurs at $y_{pe\_\max} = \sqrt{c_{pe}/2}$. We define a distance, δ_{pe}, as the range of influence of the moment profile. δ_{pe} is the distance in which the momentum is higher than 2% of its maximum value. It can be shown that $\delta_{pe} \approx 2.371\sqrt{c_{pe}}$. We define δ_{pe} as a reliable bound to have a finite time of capture. Similar analysis and definitions are valid for $g_{ep}(.)$ and δ_{ep}.

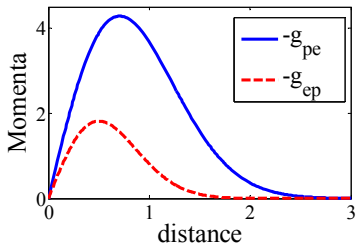

Figure 1. The momentum profiles in (1). $-g_{ep}, -g_{pe}$. $\left[b_{ep}=6,\ c_{ep}=0.5,\ b_{pe}=10,\ c_{pe}=1\right]$

The momenta profiles g_{pe} and g_{ep} are depicted in Fig. 1. The attraction moment on the pursuer is always greater than the repulsion on the evader; and the dynamics will come to a stable equilibrium at $d=0$. *Capture* is defined when $\|y\| < d_{capture} = 0.02\delta_{pe}$. This case is achieved by the parameter selection of $c_{ep} < c_{pe}$.

This observation can also be validated using the Lyapunov stability concept. The dynamics in (1) can be restated as

$$\dot{y} = g_{pe}(y) - g_{ep}(y) \tag{1a}$$

We consider a candidate Lyapunov function $V = 1/2\left(y^T y\right) > 0$. If V has a negative semidefinite time derivative, this implies $y \to 0$, and that capture will take place. That is,

$$\dot{V} = y^T \dot{y} = y^T\left(g_{pe}(y) - g_{ep}(y)\right) \tag{2}$$

For the 1P-1E scenario, y and $g_{pe}(y) - g_{ep}(y)$ vectors are collinear (*i.e.* on the same line); the only requirement for $\dot{V} < 0$ is that the vectors y and $g_{pe}(y) - g_{ep}(y)$ be of opposite direction. Accordingly, for the momentum given in Fig. 1, the dynamics will come to a stable equilibrium at $\|y\| = 0$, regardless of the starting configuration of pursuer and evader, $\|y(t=0)\| = d_s$. Thus, under certain conditions, the dynamics is Lyapunov stable and the evader is captured.

B. Multi-agent Swarms Case

The 1P-1E scenario above is now expanded to study multiple-agent pursuer and evader swarms with equal membership count (for simplicity). We adopt a two-phase approach for these interactions. *Phase* 1 treats the two swarms as single agents, making the ensemble act like a 1P-1E, with agents lumped at their respective swarm centers). This phase brings the swarms to a configuration where the two centers coincide. In *phase* 2 (the *individual pursuit*) the interaction logic enables the capture of each evader by a pursuer. The two phases of the operation are coambined under one continuous analysis as follows.

The system dynamics in (1) is now restated considering the interactions between alike and non-alike agents and pursuer control:

$$\dot{x}_i = g_{xi} = G_{Pi} + \sum_{\substack{j=1 \\ j\neq i}}^{N_p} g_{pp}(x_i - x_j) + \qquad i = 1:N_p$$
$$Trans\left(\overline{PE}\right) g_{pe}(x_i - z_{k_i}) - D_{art\_i}(x_i - z_{k_i}) \tag{3a}$$

$$\dot{z}_i = g_{zi} = G_{Ei} + \sum_{\substack{j=1 \\ j\neq i}}^{N_e} g_{ee}(z_i - z_j) +$$
$$Trans\left(\overline{PE}\right)\left\{\sum_{j=1}^{N_p} g_{ep}(x_j - z_i)\right\} \qquad i = 1:N_e \tag{3b}$$

where k_i is the index indicating the evader assigned to pursuer x_i. $D_{art\_i}(x_i - z_{k_i})$ is the control momentum to be defined later. The number of pursuers, N_p, and the number of evaders, N_e, are equal. Notation $g_{pp}(.)$ in (3a) refers to the momentum received by a pursuer due to the location of other pursuers. Likewise, $g_{ee}(.)$ in (3b) refers to the momentum received by an evader due to the other evaders. These momentum descriptions, presented in (4a and 4b), are taken from [1]. These momenta are characterized by long range linear attraction and short range bounded repulsion, but only for alike members. Using $u = (x_i - x_j)$, $v = (z_i - z_j)$ we define

$$g_{pp}(u) = -u\left(a_{pp} - b_{pp}\exp\left(-\|u\|^2 / c_{pp}\right)\right) \tag{4a}$$

$$g_{ee}(v) = -v\left(a_{ee} - b_{ee}\exp\left(-\|v\|^2 / c_{ee}\right)\right) \tag{4b}$$

Notice again the vanishing characteristics of g_{pp} and g_{ee} as $u, v \to 0$. They also show a linear attraction features as $u, v \to \infty$.

The necessary momenta for the pursuer and evader centers are given as

$$G_P = g_{PE}(\bar{x}-\bar{z})\,;\; G_E = g_{EP}(\bar{x}-\bar{z}) \qquad (5a,b)$$

where $\bar{x}_p$ and $\bar{z}_e$ are the centers of the pursuers' swarm and the evaders' swarm, respectively, and $\overline{PE}$ is the distance between them.

$$\bar{x} = \frac{1}{N_p}\sum_{i=1}^{N_p} x_i \;;\; \bar{z} = \frac{1}{N_e}\sum_{i=1}^{N_e} z_i \;;\; \overline{PE} = \left\|\bar{z}-\bar{x}\right\| \qquad (6a,b,c)$$

g_{PE} and g_{EP} are the same as (1) except for different parameters.

We then decompose these momenta to each member of the respective swarm uniformly. G_{Pi} and G_{Ei} represent the decomposed components of G_P and G_E, respectively.

The transition number, $Trans(d)$, is depicted in Fig. 2 and defined as

$$Trans(d) = \left(\frac{d_0+\delta}{2d_0+\delta}\right)\left\{1-\frac{d-d_0}{\left\|d-d_0\right\|+\delta}\right\} \qquad (7)$$

It represents the transition from *phase* 1, *i.e.*, $\overline{PE} >> d_0$, when $Trans\left(\overline{PE}\right)\cong 0$, to *phase* 2, *i.e.*, $\overline{PE} << d_0$, when $Trans\left(\overline{PE}\right)\cong 1$; d_0 is the preferred distance for transition from *phase* 1 to 2 while the parameter δ controls the smoothness of this transition function .

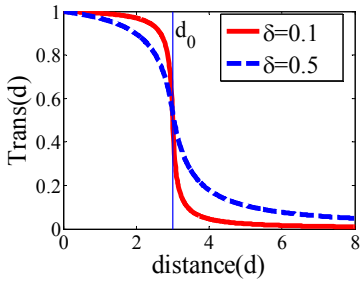

Fig. 2. Function *Trans(d), d_0=3*.

The dynamics given in (3a,b) has three features: (i) it smoothly covers the transition between *phases* 1 and 2; (ii) each pursuer has an exclusive nearest evader (ENE) assignment; (iii) there is an additional dissipative control term $-D_{art\_i}(x_i - z_{ki})$, where D_{art_i} is a positive constant (selection of which is described later). This term functions to adaptively discharge excessive energy by suppressing the over-excited behavior of the i^{th} pursuer.

The term $g_{pe}(x_i - z_{ki})$ in (3a), in fact, represents the momentum on the i^{th} pursuer by the ki^{th} evader, which is the "exclusive nearest evader", ENE, for the i^{th} pursuer. No other evader but the ENE affects this pursuer. By contrast, all pursuers influence all evaders as g_{ep} terms are under the summation in (3b).

1) Phase 1: for $\left\|\bar{x}_p - \bar{z}_e\right\| >> d_0$, $Trans\left(\overline{PE}\right)\cong 0$

$$\dot{\bar{x}} = \sum_{i=1}^{N_p}\left(G_{Pi} + \sum_{\substack{j=1\\ j\neq i}}^{N_p} g_{pp}(x_i - x_j)\right) = G_P \qquad (8a)$$

$$\dot{\bar{z}} = \sum_{i=1}^{N_e}\left(G_{Ei} + \sum_{\substack{j=1\\ j\neq i}}^{N_e} g_{ee}(z_i - z_j)\right) = G_E \qquad (8b)$$

Following the earlier 1P-1E discussion, if the momenta profiles follow those of Fig. 1, the resulting dynamics will lead to the merging of the two swarms as in the 1P-1E case. *Phase 1* has a number of characteristics:

1. The merging of the two swarms (*i.e.*, *phase* 1) occurs in a finite time if the initial distance between the two swarms is lower than the maximum recognition distance or the range of action of the pursuers momentum g_{PE}, defined previously as δ_{PE}. Otherwise, the two swarms will converge independently following the homogeneous momenta interactions, (*i.e.*, for alike members).
2. In this phase, if the approach time is larger than each of the homogeneous swarm convergence times, the size of each swarm will be dictated only by the nature of the interaction forces g_{pp} and g_{ee} for predators and evaders, respectively. This size and bounded time are evaluated in [1], but only for the case of homogeneous swarms.

a) Lyapunov Stability Analysis on Phase 1

We define the Lyapunov candidate for the center of the swarms as:

$$V_E = \frac{1}{2}\left(PE^T PE\right) \text{ with } PE = \bar{z}-\bar{x} \qquad (9)$$

By definition, this Lyapunov candidate is a positive definite function. To analyze the negativity of its time derivative

$$\begin{aligned}\dot{V}_E &= PE^T(dPE/dt) = PE^T\left(\dot{\bar{z}}-\dot{\bar{x}}\right)\\ &= PE^T(G_E - G_P) \quad \forall\ \left\|\bar{z}-\bar{x}\right\| > d_0\end{aligned} \qquad (10)$$

From (10) and earlier discussions in section II.A., when the parameter selections comply with the momenta profiles in Fig. 1, the Lyapunov candidate of (9) meets the negativity condition in its time derivative. These conditions ensure that the total repulsion momentum on evaders G_E is smaller than the total attraction momentum on pursuers G_P. During the initial phase in the swarm aggregation, the predominant forces are those that drive V_E to zero.

b) General Lyapunov function selection in Phase 1-2 Transition

The general Lyapunov candidate for the whole system in (3a,b) is selected as

$$V_G = \frac{1}{2}\left(PE^T\ PE\right) + w.Trans\left(\overline{PE}\right)\sum_{i=1}^{N_p}\frac{1}{2}\left(x_i - z_{ki}\right)^T\left(x_i - z_{k_i}\right) \quad (11)$$
$$= V_E + w.Trans\left(\overline{PE}\right)\sum_{i=1}^{N_p} V_{Gi}$$

V_E accounts for the dynamics between the centers of the pursuers and evaders swarms and V_{Gi} terms represent the individual pursuer-evader assignments. The V_E term is the most prominent during *phase* 1 ($Trans\left(\overline{PE}\right) \cong 0$) while the V_{Gi} terms are significant during *phase* 2, to be considered later. The factor *w* is a user selected normalizing constant that should be close to $1/N_p$.

2) Phase 2

Once the two swarm centers are closer than the distance d_0, *phase* 2 or individual pursuit starts. During this second phase it is assumed that $\overline{PE} << d_0$. This property is enforced because of the momenta G_P and G_E. Any departure away from this region (*i.e,*. creating $\overline{PE} > d_0$) forces $Trans\left(\overline{PE}\right)$ to diminish in (3) which, in turn, invites *phase* 1 dynamics (8) and brings $\overline{PE} \le d_0$.

Provided that $\left\|\bar{z} - \bar{x}\right\| = \overline{PE} << d_0$,we can assume that $G_{Pi} \approx 0$, $G_{Ei} \approx 0$, $Trans(\overline{PE}) \approx 1$. Therefore (3) becomes

$$\dot{x}_i = g_{xi} \approx \sum_{\substack{j=1 \\ j\neq i}}^{N_p} g_{pp}(x_i - x_j) + g_{pe}(x_i - z_{k_i}) - D_{art\_i}(x_i - z_{k_i}) \qquad i = 1:N_p \quad (12a)$$

$$\dot{z}_i = g_{zi} \approx \sum_{\substack{j=1 \\ j\neq i}}^{N_e} g_{ee}(z_i - z_j) + \sum_{j=1}^{N_p} g_{ep}(x_j - z_i) \qquad i = 1:N_e \quad (12b)$$

where z_{ki} is again the exclusive nearest evader (ENE) to pursuer x_i, selected globally to avoid more than one pursuer chasing the same evader in (12a); in *phase* 2, each pursuer prosecutes an assigned evader. On the other hand, the evaders still try to avoid all the pursuers in (12b). With this pursuer-evader assignment we study the stability of the dynamics next.

III. Lyapunov Based Energy Dissipation

In *phase* 2 each evader avoids all the pursuers. Therefore, the simple necessary condition for Lyapunov stability in *phase* 1, $c_{ep} < c_{pe}$ will no longer suffice. The pursuer-ENE dynamics may be destabilized due to the influence of the other pursuers. To ensure stability, we inject an energy dissipating (*i.e.* damping) term in the control momenta on the pursuers, (12a), $D_{art\_i}(x_i - z_{k_i})$.

The artificial damping constant D_{art_i} is selectively imposed on the pursuers only. This constant is responsible for maintaining the negativity of $\dot{V}_G$. The following computational scheme is used for selecting this constant.

i. As we monitor V_G numerically, we compute the two successive values for the current and the previous step, $V_G(k)$ and $V_G(k-1)$.
ii. If $V_G(k) \le V_G(k-1)$, $D_{art\_i} = 0 \ \ \forall\ i = 1:N_p$ and no damping is applied to any pursuer.
iii. If $V_G(k) > V_G(k-1)$ then the control discharges enough energy in the following step to revert this increase. For this, our routine first identifies the pairs of $(x_i - z_{k_i})$ which cause the increase in V_G.

Considering the general dynamics, from (12a,b)

$$\frac{d}{dt}\left(x_i - z_{k_i}\right) = \frac{d}{dt}(y_i) = f_i(x,z) - D_{art\_i}(x_i - z_{k_i}) \quad (13)$$

Lemma. Consider the dynamics given in (13) where $f_i(x,z)$ is slowly varying with respect to the control sampling speed. The dissipative term given by D_{art_i}, can be selected adaptively such that it enforces the reversal of increase of the Lyapunov function in one sampling step.

Proof. Assume that $\left\|y_i\right\| = \left\|x_i - z_{k_i}\right\| \quad \forall\ i = 1:N_p$ displays an increase from step *k-1* to *k* and in turn $V_G(k) > V_G(k-1)$ occurs. If one takes $f_i(x,z) \approx$ constant , it enforces an increment of $\Delta\left\|y_i\right\|$ per sampling step *h*. The term $D_{art\_i}(x_i - z_{k_i}) = D_{art\_i}\, y_i$ is expected to remove this $\Delta\left\|y_i\right\|$ in one step from *k* to *k+1*, while $f_i(x,z)$ exerts another Δy_i in the same interval. We propose the selection of D_{art_i} such that it enforces a $2\Delta\left\|y_i\right\|$ decrease to compensate for the act of $f_i(x,z)$ over two steps. Notice that the damped portion of the dynamics is

$$\dot{y}_i = -D_{art\_i}\, y_i \qquad or \qquad \frac{d}{dt}(\ln y_i) = -D_{art\_i} \quad (14)$$

One step integration of (14) from *t(k)* to *t(k+1)*, *i.e.*, *h* seconds, results in

$$\ln\left(\frac{y_i(k+1)}{y_i(k)}\right) = -D_{art\_i}\, h .$$

On the other hand $\frac{y_i(k+1)}{y_i(k)} = \sqrt{\frac{V_{Gi}(k+1)}{V_{Gi}(k)}}$. Thus we select

$$D_{art\_i} = \frac{1}{h}\ln\sqrt{\frac{V_{Gi}(k)}{V_{Gi}(k+1)}} \quad (14a)$$

Because the desired outcome is to bring $V_{Gi}(k+1)$ to the level of $V_{Gi}(k-1)$ despite the continuing effect of $f_i(x,z)$ during *k* to *k+1* controlled step, we impose

$$D_{art\_i} = \frac{1}{h}\ln\frac{V_{Gi}(k)}{V_{Gi}(k-1)} \qquad (15)$$

This dissipative control action is capable of assuring $\dot{V}_{Gi} < 0$ end result. QED.

Several further improvements are made on the damping selection:

- Piecewise enforcement of the Lyapunov function. If $V_G(k) > V_G(k-1)$ occurs following a new pursuer-ENE assignment, we simply ignore this increase and select $D_{art\_i} = 0 \;\; \forall \; i = 1:N_p$. We continue monitoring the V_G variation during the following simulation steps and deploy D_{art_i} as suggested in (15) if needed; this monitoring is done every simulation step until a new ENE assignment occurs. The Lyapunov candidate exhibits negative time derivative (except at the instants of new ENE assignments). Such piecewise continuous Lyapunov function still guarantees the system stability, which means capture of the evader by the pairing pursuer.
- If $V_G(k) > V_G(k-1)$ and the component for the swarm centers dynamics V_E is also increasing, a damping control is computed, following (15). The control is distributed on all the pursuers evenly as increments in all the D_{art_i} terms.

These steps assure the Lyapunov stability for both *phase* 1 and 2.

IV. Simulation Results and Performance Tests

In this section we present a case study which represents some interesting properties of the proposed swarm control logic. It is a 6P-6E scenario with a randomly selected initial swarm setting, which uses the same momenta profiles as prescribed in Table I.

Fig. 3(A-D) presents the simulation results divided in four panels. Sets A and B are for the damped and undamped systems, respectively. The frames labeled A_1 and B_1 illustrate the time history of the Lyapunov candidate function, black dots mark the times of new assignment of ENE. Middle frames, labeled A_2 and B_2, show the instants

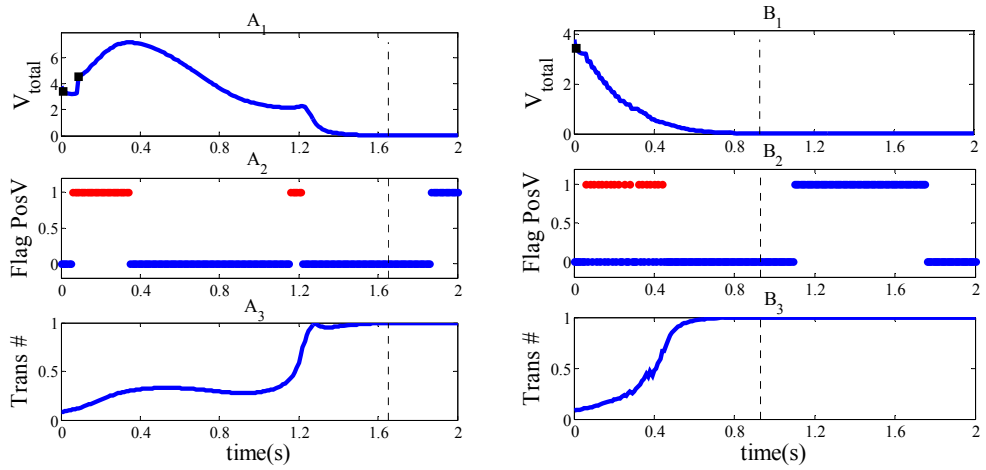

Fig. 3. Simulation Results. 3A: Using undamped control logic. 3B: Using damped control logic.

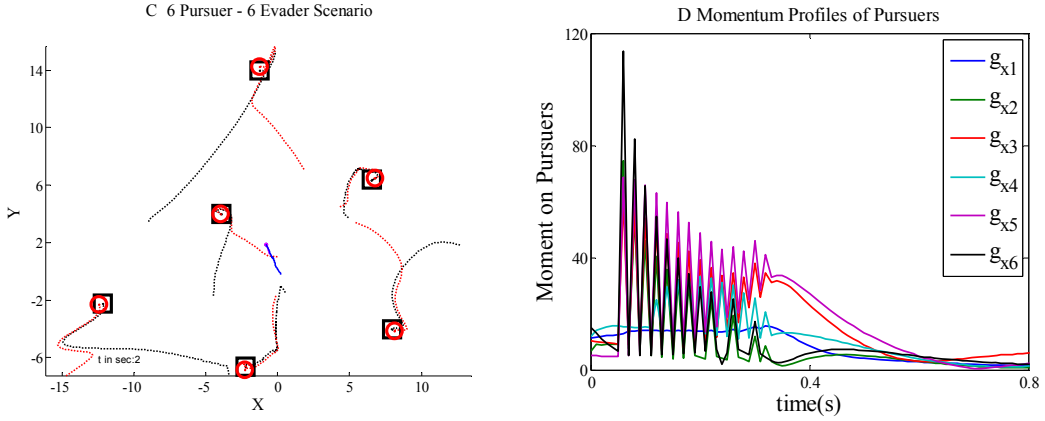

Fig. 3 (Cont). Simulation Results. 3C: Damped swarm pursuit.3D: Total momenta on each pursuer

where Lyapunov violations occur (*i.e.,* $V_G(k) > V_G(k-1)$. Red marks at a value of "1" indicate violations before capture and the blue dots at a value of "1" indicate violations after capture. Blue dots at value of "0" indicate no violation, *i.e.*, $V_G(k) \le V_G(k-1)$. Bottom frames, labeled A_3 and B_3, present the time history of the transition number, $Trans(\overline{PE})$, signaling how fast the swarms merge in *phase* 1.

The vertical dotted line in panels A and B indicate the time of capture, defined as the instant in which all the distances between each pursuer and its assigned ENE are smaller than $d_{capture}$.

TABLE I
PARAMETRIC PROPERTIES OF THE CASE STUDY

$a_{ee} = 0.1$	$a_{pp} = .1$	$B_{EP} = 10$	$\delta = 0.2$
$b_{ee} = 30$	$b_{pp} = 40$	$C_{EP} = 25$	$d_0 = 0.25$
$c_{ee} = 20$	$c_{pp} = 5$	$B_{PE} = 35$	w=1/6
$b_{ep} = 20$	$b_{pe} = 25$	$C_{PE} = 30$	
$c_{ep} = 10$	$c_{pe} = 30$		

Fig. 3A1 is the Lyapunov function without damping control. At *t = 0.08 s.*, a change in assigned ENE (denoted by the black dots in Fig. 3A1) results in a jump in the Lyapunov function. Afterwards, the function continues to increase until *t=0.34 s*. Another increase is found at $t = 1.16s$. This increase is due to the pursuers being far away from their ENEs as phase 2 takes over.

Despite piecewise violations of the Lyapunov stability conditions (*i.e.,* $\dot{V}_G < 0$ violation) the process ultimately reaches capture (*i.e.,* $V_G \cong 0$) as shown in Fig. 3A1 at about $t = 1.6s$

We then deploy the damping control to prevent $\dot{V}_G < 0$ violations, as shown in Figs. 3B(1-2-3). The Lyapunov function exhibits a continually decreasing trend. Although it does increase at some instants (between *0.05 s and 0.44 s.*), the introduced damping control enforces the Lyapunov function to decrease in one sampling step. In short, $\dot{V}_G < 0$ is maintained throughout except appearing in one-time-step intermittent excursions as shown by the flags in Fig. 3B2.

Notice that for *1.1< t < 1.7 s*., the violations of $\dot{V}_G < 0$ condition are caused by residual and ignorable oscillatory motion in pursuer and evaders which yield only ignorable increase in V_G. Therefore, damping control is not deployed. We notice in the traces of Fig. 3C, the capture takes place around $t = 0.9\,s$ as pursuers (marked by squares) and the evaders (red circles), coincide. Fig. 3D shows the total momenta on each of the pursuers. Chatter in the momenta only takes place in single-time-step pulses to negate the trend of $\dot{V}_G > 0$. There is a need to smoothen the momenta; which is a goal for our ongoing research.

V. DISCUSSION AND CONCLUSION

We present a control strategy for a dynamics involving two equal-strength swarms which are in conflict. Lyapunov based control law imposes the ultimate capture of the evaders. The strategy has two phases: *phase* 1 is to bring the swarms closer and *phase* 2 is for the individual pursuit of a designated evader by each pursuer.

The simulation of these strategies leads to the conclusion that the capture takes place. A condition to obtain successful capture is that the initial configuration of the swarms should have centers closer than the parameter δ_{PE}, or range of action of the pursuer's momentum profile.

The proposed general Lyapunov candidate behaves as expected until the end of *phase* 1, which was demonstrated to have negative time derivative. After *phase* 1, an artificial damping control in the pursuers will guarantee that the function will always decrease except for excursions appearing due to the reassignment of ENE. This behavior does not disrupt the piecewise deployment of Lyapunov stability.

REFERENCES

[1] V. Gazi and K. M. Passino, "Stability analysis of swarms," *IEEE Trans Autom Control,* vol. 48, pp. 692-697, 2003.

[2] V. Gazi and K. M. Passino, "Stability analysis of social foraging swarms," *IEEE Transactions on Systems, Man, and Cybernetics, Part B: Cybernetics,* vol. 34, pp. 539-557, 2004.

[3] S. Camazine, J. -. Deneubourg, N. R. Franks, J. Sneyd, G. Theraulaz and E. Bonabeau, *Self-Organization in Biological Systems,* 2001.

[4] T. Vicsek, A. Czirk, E. Ben-Jacob, I. Cohen and O. Shochet, "Novel type of phase transition in a system of self-driven particles," *Physical Review Letters,* vol. 75, pp. 1226-1229, 1995.

[5] T. Chu, L. Wang and T. Chen, "Self-organized motion in anisotropic swarms," *Journal of Control Theory and Applications,* vol. 1, pp. 77-81, 11/01/. 2003.

[6] T. Chu, L. Wang, T. Chen and S. Mu, "Complex emergent dynamics of anisotropic swarms: Convergence vs oscillation," *Chaos, Solitons & Fractals,* vol. 30, pp. 875-885, 11. 2006.

[7] S. Chen, L. Zhao and Y. Han, "Multi-agent aggregation behavior analysis: The dynamic communication topology," *J. Syst. Sci. Complex.,* vol. 21, pp. 209-216, 2008.

[8] J. Yao, R. Ordóñez and V. Gazi, "Swarm tracking using artificial potentials and sliding mode control," *J Dyn Syst Meas Control Trans ASME,* vol. 129, pp. 749-754, 2007.

[9] L. Chaimowicz, V. Kumar and M. F. M. Campos, "A Paradigm for dynamic coordination of multiple robots," *Autonomous Robots,* vol. 17, pp. 7-21, 07/01/. 2004.

[10] C. Belta and V. Kumar, "Abstraction and control for Groups of robots," *Robotics, IEEE Transactions on,* vol. 20, pp. 865-875, 2004.